Environmental Pollution 158 (2010) 711–722

Contents lists available at ScienceDirect

Environmental Pollution

journal homepage: www.elsevier.com/locate/envpol

High-resolution inventory of NO emissions from agricultural soils over the Ile-de-France region

M.-N. Rolland [a,1], B. Gabrielle [a,*], P. Laville [a], P. Cellier [a], M. Beekmann [b], J.-M. Gilliot [a], J. Michelin [a], D. Hadjar [a], G. Curci [c]

[a] INRA, AgroParisTech, UMR 1091 Environnement et Grandes Cultures, F-78850 Grignon, France
[b] Laboratoire Inter-universitaire des Systèmes Atmosphériques – CNRS, Universités Paris-Est and Paris 7, F-94 010 Créteil, France
[c] Dipartimento di Fisica – CETEMPS, Universita' degli Studi dell'Aquila, 67010 Coppito, L'Aquila, Italy

The use of an agro-ecosystem model at regional scale makes it possible to map the emissions of nitric oxide from arable soils at a resolution compatible with tropospheric ozone models.

ARTICLE INFO

Article history:
Received 24 May 2009
Received in revised form
10 October 2009
Accepted 13 October 2009

Keywords:
Ecosystem models
CERES
Nitric oxide
Ozone
Arable soils
Emission map
Regional scale

ABSTRACT

Arable soils are a significant source of nitric oxide (NO), a precursor of tropospheric ozone, and thereby contribute to ozone pollution. However, their actual impact on ozone formation is strongly related to their spatial and temporal emission patterns, which warrant high-resolution estimates.

Here, we combined an agro-ecosystem model and geo-referenced databases to map these sources over the 12 000 km^2 administrative region surrounding Paris, France, with a kilometric level resolution. The six most frequent arable crop species were simulated, with emission rates ranging from 1.4 kg N–NO ha^{-1} yr^{-1} to 11.1 kg N–NO ha^{-1} yr^{-1}. The overall emission factor for fertilizer-derived NO emissions was 1.7%, while background emissions contributed half of the total NO efflux. Emissions were strongly seasonal, being highest in spring due to fertilizer inputs. They were mostly sensitive to soil type, crops' growing season and fertilizer N rates.

1. Introduction

Although agricultural soils have been recognized as a significant source of nitric oxide (NO), their contribution is still uncertain, ranging from 10% to 23% of the global NO_x budget (Davidson and Kingerlee, 1997; Delmas et al., 1997), with a 15% share in Europe (Simpson et al., 1999). They may play a significant role in the tropospheric chemistry of ozone (O_3) in rural areas, where NO_x emissions from combustion sources are relatively small. This also holds in the vicinity of urban areas, where arable soils are tightly intertwined with other sources of ozone precursors such as road traffic, forests, or residential and industrial areas. Photochemical processes are highly dependent on the spatial and temporal patterns of natural and anthropogenic sources of ozone precursors, and their simulation warrants high-resolution estimates of these sources in both space and time.

In arable soils, NO is produced through the microbial processes of nitrification and denitrification. Nitrification is an oxidation of NH_4^+ to NO_2^- and NO_3^-, which requires the availability of molecular oxygen, while denitrification is an anaerobic reduction of NO_3^- to gaseous forms of N (N_2O and N_2). The nitrification pathway predominates in temperate zones (Laville et al., 2005), accounting for 60–90% of total NO emissions (Godde and Conrad, 2000), and is regulated by environmental and agronomic factors including cropping practices, soil characteristics and climate. Crop management influences the dynamics of soil ammonium content, which is a substrate for nitrification, while the latter influence soil temperature and water-filled pore space (WFPS), which is a proximate for soil oxygen concentration and a driver for gaseous diffusivity (Linn and Doran, 1984).

Given the complexity of the microbial processes driving the exchanges of reactive N (Nr) between soils and the atmosphere, estimates of biogenic sources remain highly uncertain at regional to global scales. National inventories of Nr sources from ecosystems currently mostly rely on sets of emission factors derived from field-scale experiments, assuming Nr emissions to be a fixed fraction of Nr inputs or dependent solely on soil temperature. Such is the case

* Corresponding author at: INRA, AgroParisTech, UMR1091 Environnement et Grandes Cultures, Route de Thiverval BP 01, 78850 Thiverval-Grignon, France. Tel.: +33 1 30 81 55 51; fax: +33 1 30 81 55 63.
E-mail address: Benoit.Gabrielle@agroparistech.fr (B. Gabrielle).
[1] Present address: Numtech, F-63175 Aubière, France.

0269-7491/$ – see front matter © 2009 Elsevier Ltd. All rights reserved.
doi:10.1016/j.envpol.2009.10.017

Table 1
Areas and management practices for the 6 dominant crop types and fallow soils in the Ile de France region. Dates are given as days of year (year).

Crop type	Area (ha)	Management practices			
		Sowing	Fertilizer application		
		Date	Date	Rate[a]	Form
Maize (*Zea mays* L.)	43 144	107(2001)	115 (2001)	140	UAN[b]
Wheat (*Triticum aestivum* L.)	256 974	295 (2000)	63 (2001)	60	UAN[b]
			93 (2001)	100	AN[c]
Barley (*Hordeum vulgare* L.)	60 162	289 (2000)	54 (2001)	60	UAN
			92 (2001)	100	UAN
Rapeseed (*Brassica napus* L.)	52 015	251 (2000)	29 (2001)	60	AN
			51 (2001)	120	AN
Pea (*Pisum sativum* L.)	32 278	98 (2001)	none		
Sugarbeet (*Beta vulgaris* L.)	41 727	112 (2001)	29 (2001)	40	AN
			58 (2001)	89	AN
Fallow soils[d]	38 711	240 (2000)	none		

[a] Unit: kg N ha^{-1}.
[b] UAN: nitrogen solution (50% urea and 50% ammonium-nitrate, in liquid form).
[c] AN: ammonium-nitrate.
[d] Simulated as a mustard catch crop, ploughed in date on day of year 182 (2001).

for the widely-used EMEP/CORINAIR methodology (Skiba et al., 2001; Stohl et al., 1996).

In recent years, biophysical ecosystem models have been used to develop more realistic, spatially-explicit inventories of gaseous Nr emissions from soils, based on specific geographical information systems (GIS) and databases (Butterbach-Bahl et al., 2001, 2004, 2009; Li et al., 2004; Gabrielle et al., 2006b). Such models make it possible to simulate the temporal and spatial dynamics of emissions, typically on a daily basis. Geo-referenced databases are used to localize the sources of Nr emissions, as well as to map model inputs, including soil characteristics, land-use and management, and weather data. They are used in a wide range of scientific fields, including climatology and climate change studies, agriculture, forestry and ecology (Chapman and Thornes, 2003). For instance, the DNDC and PnET-N-DNDC models were used to develop regional inventories NO and N_2O emissions from cropland and forests in various parts of the world (Butterbach-Bahl et al., 2001, 2004; Li et al., 2004; Kiese et al., 2004). In these studies, the spatial generalization at the regional scale was based on plot-scale simulations at the nodes of a regular grid involving particular sets of crop management, soil, and climate data. Spatial interpolation of the grid points to cover the entire domain was either not considered (implying the points were representative of the whole grid cell), or done using kriging techniques. The density of the grid points (with a grid resolution of 4–20 km) was generally too low to adequately capture the short-range variations in agricultural field properties, which are in the 0.1–1 km range.

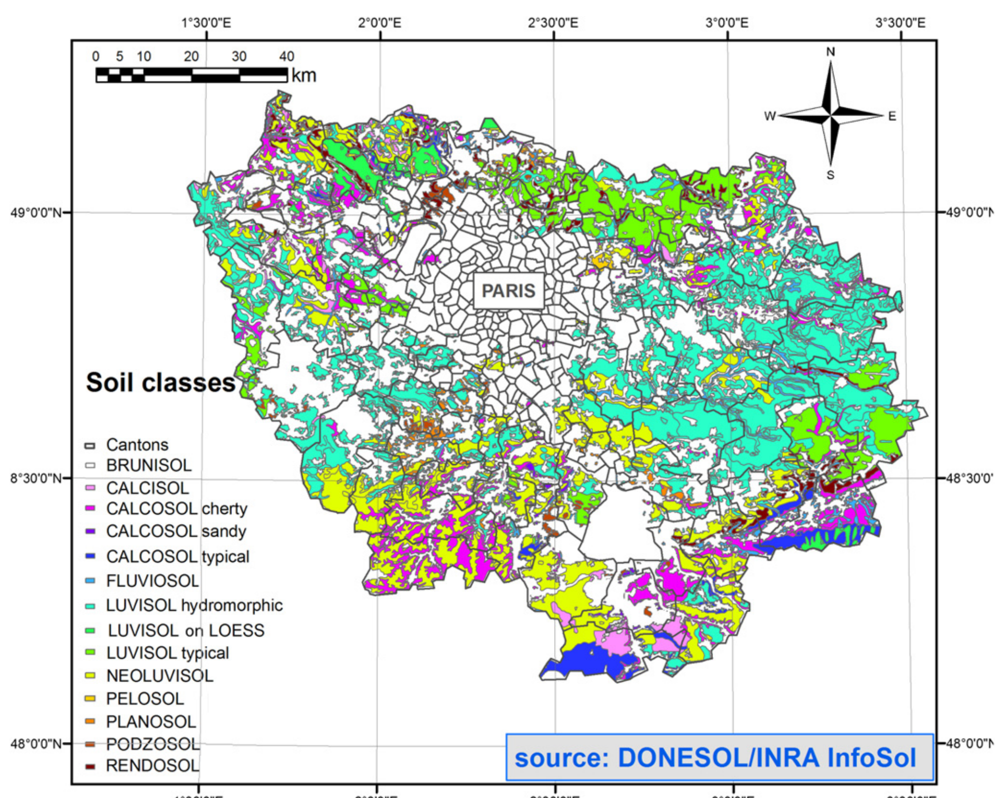

Fig. 1. Soil map units as overlaid with administrative county limits and the presence of arable crops in the Ile de France region.

Table 2
Groups of dominant soil types defined for the Ile de France region.

Soil group (Baize and Girard, 1998)	Drainage characteristics	Geological substrate	Texture	Reference
Brunisol	well-drained, hydromorphic	variable	sandy to clayey	created
Calcisol	well-drained	limestone	clay loam	(Gabrielle et al., 2002)
Calcosol, cherty	well-drained	limestone or chalk	clay loam	(Roche et al., 2001)
Calcosol, sandy	well-drained	limestone	silt sandy	created
Calcosol, typical	well-drained	limestone or chalk	silty	created
Fluviosol	well-drained	alluvial deposits	silty	created
Luvisol on loess	well-drained	loess	clay loam	(Hermel, 2001)
Luvisol, hydromorphic	hydromorphic	clay	clay loam	(Gabrielle et al., 2002)
Luvisol, typical	well-drained	limestone	clay loam	(Gabrielle et al., 2002)
Neoluvisol	well-drained	limestone	clay loam	(Gabrielle et al., 2002)
Pelosol	very hydromorphic	clay	clay	created
Planosol	very hydromorphic	clay	silty or sandy/clayey	created
Podzosol	very well-drained	sand	sandy	(Gabrielle et al., 1998)
Rendosol	well-drained	limestone	clay loam	(Gabrielle et al., 1998)

An alternative approach consists of using over vectorial contours, delineated by the geographical borders of soil and land-use classes, as well as administrative zones. This makes it possible to encompass the range of soils, land-uses and climates occurring over the entire geographical zone considered, and not only their particular realizations at the nodes of a regular grid. Such was the basis of the N_2O inventory developed by Gabrielle et al. (2006b) for wheat-cropped soils in northern France, which resulted in principle in a more accurate localization of emission sources compared to grid-point simulations. The spatial distribution of meteorological data, which are input to biophysical models, is also an issue given their short-range variability. They are mostly taken from ground-based stations (Monestiez et al., 2001), and less frequently from global or meso-scale meteorological models (Bardossy and Plate, 1992). The latter allow a higher resolution in time and space, typically down to the hourly and 6 km scale, and provide a more regular rendering of weather patterns over a given area (Faivre et al., 2004).

Achieving a vectorial, high-resolution inventory for NO emissions from arable soils is paramount to understanding and predicting their effects on tropospheric chemistry, especially in urbanized areas where the sources of precursors are tightly intertwined. This is clearly not the case in current chemistry-transport models (CTM), which rely on fixed, biome-specific emission factors, such as the Stohl et al. (1996) or Yienger and Levy (1995) algorithms. These models may thus benefit from the recent progresses in the prediction of NO emissions by ecosystem models. However, none of the earlier above-mentioned studies in that direction had a spatial resolution compatible with the short-range (1–10 km) variations of the characteristics of arable soils and crop management.

Here, we set out to produce a high-resolution map of NO emissions from agricultural soils with the environmentally-oriented agro-ecosystem model CERES-EGC (Gabrielle et al., 2006a). Our main objective was to improve the resolution of agricultural NO sources that could be used in chemistry-transport models (CTM) to better reproduce ozone concentrations. The domain area was the Ile de France administrative region (12 072 km^2), surrounding Paris, France, which faces significant tropospheric ozone pollution (Deguillaume et al., 2008). We first overlaid a set of regional GIS databases to provide model input files at the county level across Ile de France, and ran spatially-distributed simulations of the 6 main arable crops with CERES-EGC, over a 14-month timeframe. We analysed the effects of the main physical and management drivers on the temporal and spatial patterns of NO emissions, using the regional maps and complementary multi-factorial sensitivity analyses. The regional emissions were compared to other estimates of agricultural source strength, and to simpler NO emission algorithms currently used in CTM.

2. Material and methods

2.1. *The CERES-EGC model*

CERES-EGC was adapted from the CERES family of soil-crop models, with a focus on the simulation of environmental outputs such as nitrate leaching and gaseous emissions of ammonia and nitrogen oxides (Gabrielle et al., 2006a). CERES-EGC contains submodels for the major processes governing cycles of water, carbon and nitrogen in soil-crop models. A physical module simulates the transfer of heat, water and nitrates down the soil profile as well as soil evaporation, plant water uptake, and transpiration in relation to climatic conditions. A microbiological module simulates the turnover of organic matter in the plough layer, involving both mineralization and immobilization of mineral N (denitrification and nitrification). CERES-EGC includes a submodel that simulates the production of NO through the nitrification pathway (Rolland et al., 2008). Nitrification is modeled as a Michaëlis–Menten reaction, with NH_4^+ as substrate, as modulated by soil water content and temperature. The fraction of nitrified ammonium evolved as NO is considered fixed for a given crop type (Laville et al., 2005). CERES-EGC runs on a daily time step, and requires daily rain, mean air temperature and Penman potential evapo-transpiration as forcing variables.

2.2. *Regional simulations*

We simulated NO emissions from agriculture over the Ile de France region (12072 km^2), ie an approximately 150 km $\times$ 150 km square area surrounding Paris, France. The region is characterized by a variety of land-uses, among which the share of agricultural and forest soils is 55% and 23%, respectively. A GIS database was constructed with available geo-referenced data on the region, including administrative borders, land-cover type, crop management practice, soils and climate. The corresponding layers of spatial information were mostly in vector format, and overlaid to delineate elementary spatial units representing unique combinations of soil types, weather pattern, and agricultural management. These units were subsequently used in the CERES-EGC simulations at the field-scale, in a bottom-up approach to map the emissions.

2.2.1. *Land-use and crop management*

Geographical information concerning land-use in Ile de France were taken from the *Corine Land Cover* database (thereafter referred to as CLC2000 – UE-Ifen CLC 2000; IFEN, 2005), which includes 44 classes, with a 150 m positioning accuracy and a minimum mapping unit of 25 ha. It thus allowed a precise localization of arable fields. Agricultural statistics on the area of arable crops on a county ('canton') basis were taken from the statistics and survey bureau of the French Ministry of Agriculture (SCEES), as obtained from a comprehensive census carried out from October 2000 to March 2001. Informations of agricultural cropping practices were available at the regional scale, from a detailed survey (Agreste/SCEES, 2001), including statistics on sowing dates, the dates, forms and rates of fertilizer applications, and crop yields.

The agricultural statistics showed that six crop types and fallow soils accounted for 91.5% of the total area of arable land (573 590 ha) in the Ile de France region in 2001. Table 1 summarizes their management, as taken from the above-mentioned surveys. The CERES-EGC model was run for these 6 crop species, and fallow was simulated as a mustard catch-crop (ie a rotational fallow, which was the most frequent form).

2.2.2. *Soils*

Soils were parameterized based on a 1:250 000 scale map and attached thematic database (Fig. 1). The map is organized into geographical soil map units (SMU), containing a mixture of soil typological units (STU), following the model of the soil map of the European Union (King et al., 1994). In order to reduce the number

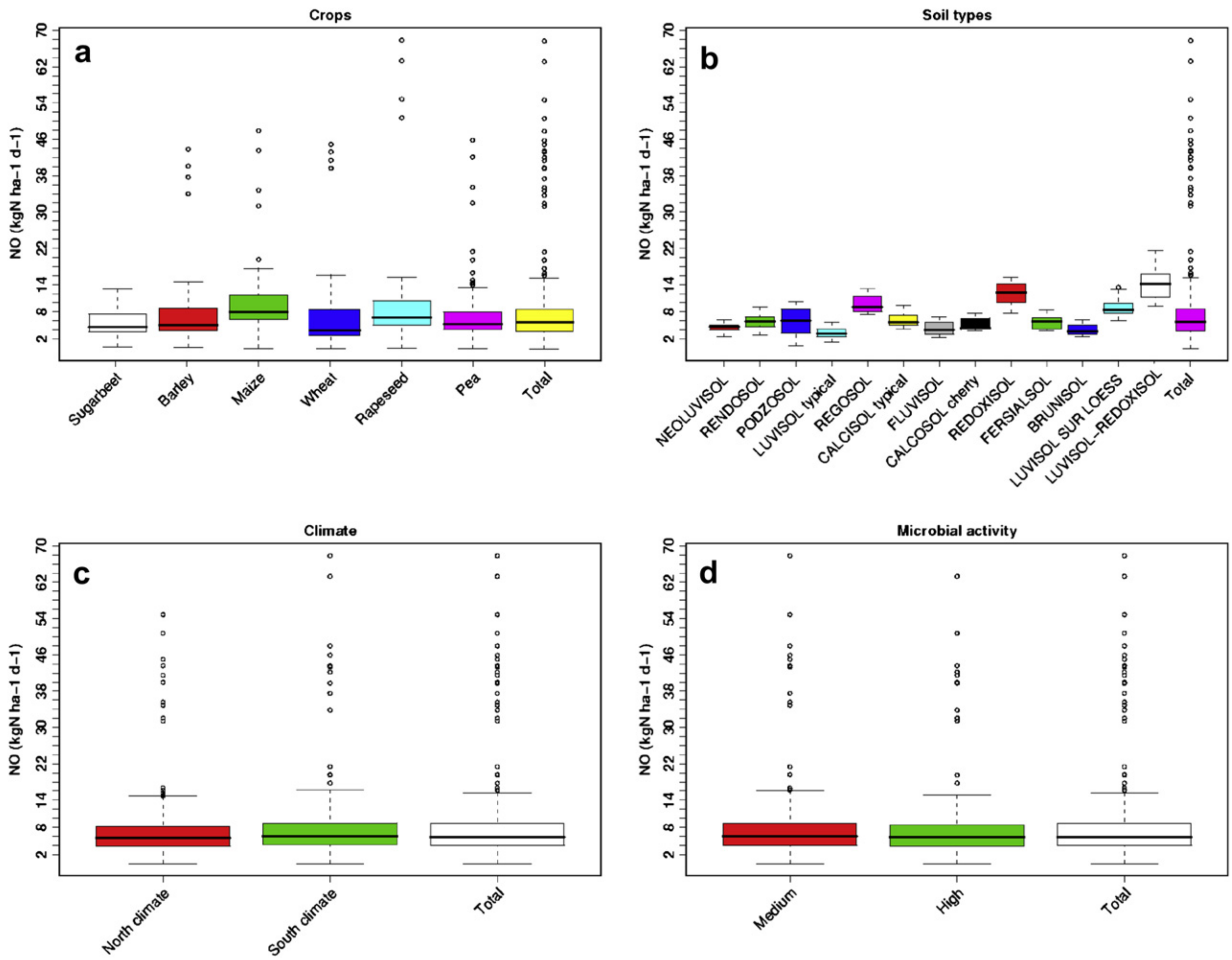

Fig. 2. Boxplots of marginal distributions for each class of data inputs: crop types (a), soil types (b), weather stations (c) and microbiological parameters (d). The boxplot of the overall distribution of NO emissions is also depicted, showing the median (solid line), first and third quartile (limits of colored rectangles), and 10th and 90th percentiles (error bars).

of soil units to be parameterized, we first selected the dominant ones in Ile de France, as determined from their percentage of land-cover on a county basis. Secondly, we grouped STUs according to their drainage class, geological substrate, and their texture class. These characteristics were considered particularly influential in the prediction of NO emissions, as evidenced by the sensitivity analysis (Section 3.1). We ultimately obtained 14 groups of soils, as listed on Table 2 and mapped out on Fig. 1. They were parameterized based on previous tests against field experimental data with CERES-EGC, involving similar soil classes in Europe (Table 2). When such prior information was unavailable, the CERES-EGC soil input file was created from the information listed in the soil database, using pedo-transfer functions and expert knowledge (Gabrielle et al., 2002).

2.2.3. Climate

CERES-EGC was supplied with gridded weather data generated by the meso-scale model MM5 (Dudhia, 1993), with a horizontal resolution of 5 km. Each CERES-EGC elementary spatial simulation unit was associated with the closest MM5 grid point for weather data. Potential evapo-transpiration (PET) was calculated from the MM5 data using the Penman relationship (Penman, 1948).

CERES-EGC was run from 1 November 2000 to 31 December 2001 for each elementary spatial simulation unit representing a given set of soil type, climate and crop management (Fig. 1). This period encompassed the growing cycles of both winter and spring crops, and the interval between harvest and sowing of the following crops.

2.3. Sensitivity analysis

As the data used in the GIS database were simplified or aggregated compared to their original format, some uncertainty is likely to have been produced during the upscaling process (Butterbach-Bahl et al., 2004; Li et al., 2004). We addressed it by examining the sensitivity of the simulated NO efflux to soil, meteorological, and crop management inputs. Sensitivity tests were first run at the plot-scale, using a complete experimental design to simultaneously vary crop type, fertilizer N rate, soil type, soil microbiological parameters, and weather data. The crop and soil types corresponded to those occurring in Ile de France (Table 2), while two climatic locations were tested: Grignon (west of Ile de France) and Auradé (Southwestern France). Two values for the microbiological parameter V_{max} (maximum nitrification rate) were taken from a previous modeling study on NO emissions (Rolland et al.,

Table 3
Sensitivity indices derived from the ANOVA table of the simulated NO emissions as a function of the various factors included in the plot-scale sensitivity analysis. They are calculated as the ratio of the marginal (main effect or first-order interactions) to total variances of NO fluxes. Parameter V_{max} is the maximum nitrification rate in soil (2 levels).

Input factors	Sensitivity index
Soil type	0.784[a, ***]
Crop type	0.039[***]
Climate	0.001[***]
V_{max}	0.001[***]
Soil:Crop	0.155[***]
Soil:Climate	0.005[***]
Soil:V_{max}	0.002[***]
Crop:Climate	0.001[***]
Crop:V_{max}	2.4E-5
Climate:V_{max}	2.4E-11
Residual	0.011

[***] denotes a 0.01% significance level (F-test).
[a] Significance level (*F*-test): 0.01%.

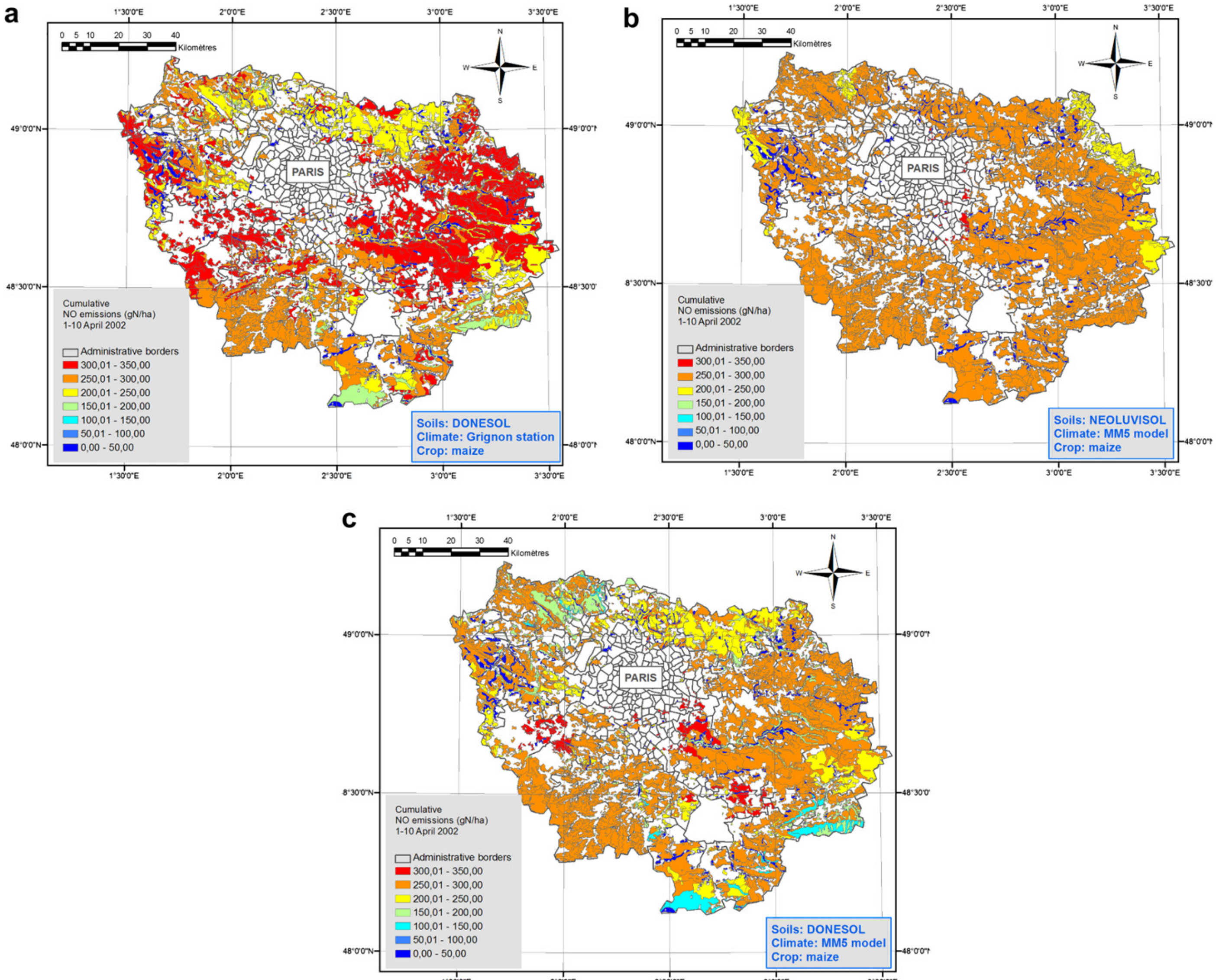

Fig. 3. Influence of physical input data on the simulated spatial patterns of NO emissions over a short period (1–10 April 2001): (a) uniform weather data taken from a ground meteorological station and soil map, (b) gridded MM5 weather data and uniform soil type (Neoluvisol), and (c) MM5 data and soil map.

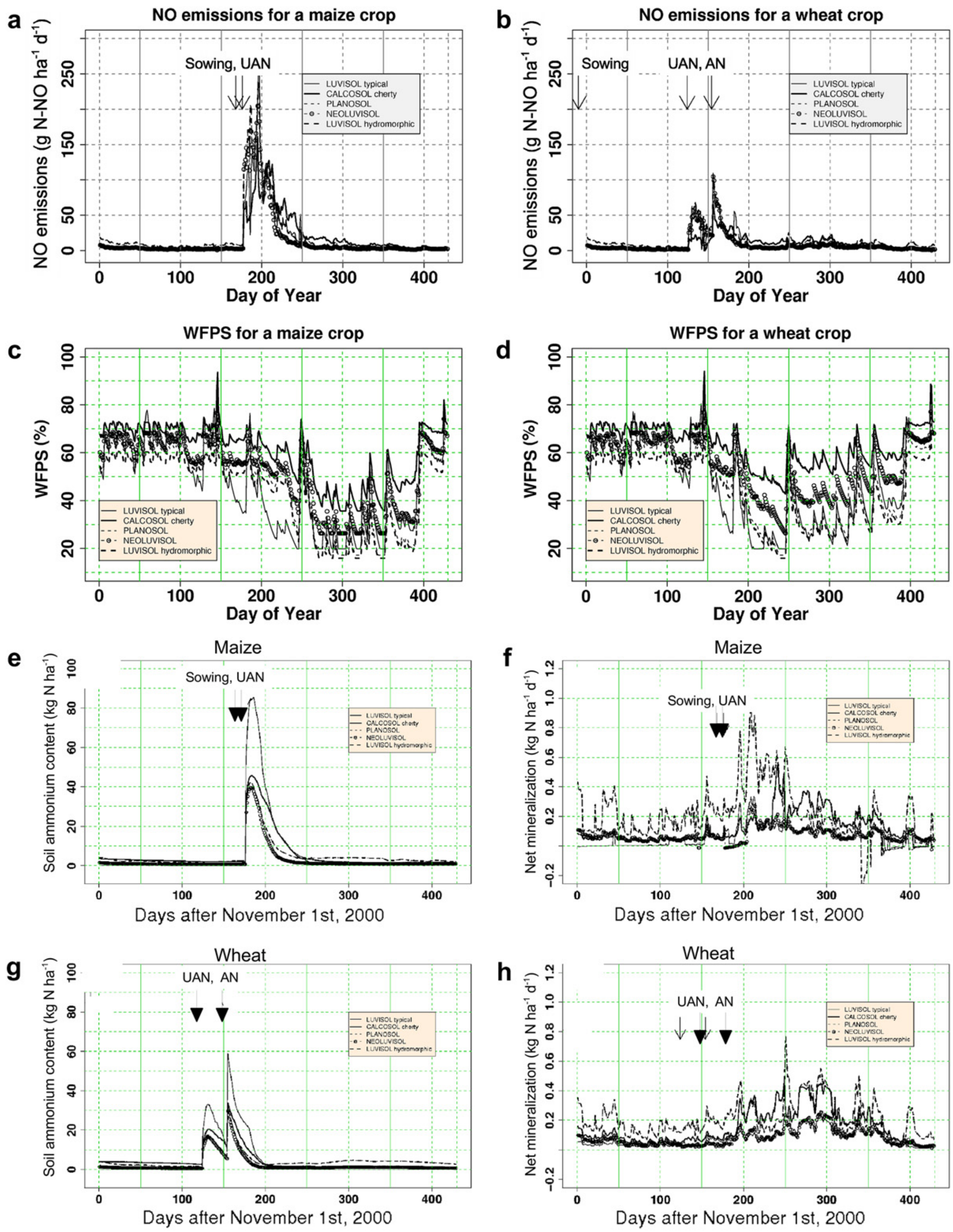

Fig. 4. Dynamics of NO emissions (a–b) and drivers: water-filled pore space (c–d), ammonium (e–f), and net N mineralization (g–h), under a similar climate (Grignon county), for a spring crop (maize) and a winter crop (wheat) and 5 soil types.

2008). They were varied independently of soil type since they had a strong influence on predicted NO emissions and little relation to soil pedological class (Cortinovis, 2004). The sensitivity of the yearly NO efflux to the above factors was assessed using boxplots, which provide a graphical representation of the distribution of model outputs, and variance analysis. The latter breaks down the total variance of model outputs into fractions attributable to individual factors and their interactions (Monod et al., 2006).

At the regional scale, the sensitivity of NO emission maps to the resolution of input data was also investigated over a short period from April 1st to 10th, 2001. This period corresponded to the peak emission rates of winter crops due to the availability of fertilizer-derived N in soils, and temperature and rainfall regimes conducive to nitrification. Three maps were compared, obtained with: i/spatially-distributed meteorological and soil data, ii/uniform weather data (Grignon meteorological station) and soil map, and iii/distributed meteorological data and uniform

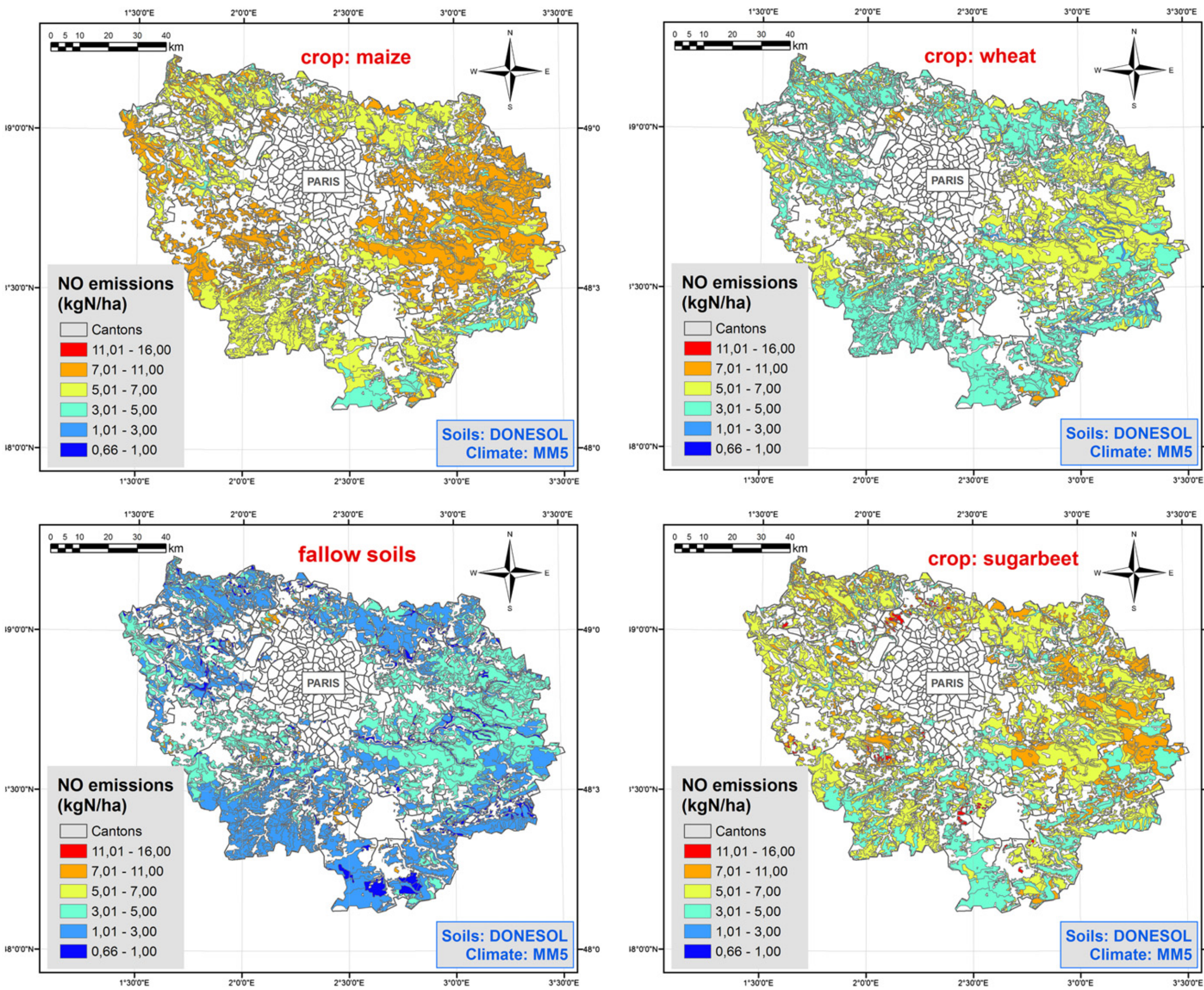

Fig. 5. Maps of cumulated NO emissions from November 2000 through December 2001, for 4 land-use types.

soil (Neoluvisol; Table 2). Lastly, the response of year-round NO emissions to N fertilizer rates was examined by varying the latter from 0 to 200 kg N ha^{-1} in 50 kg N ha^{-1} increments, encompassing the range of rates applied in Ile de France.

3. Results and discussion

3.1. Sensitivity of NO emissions to physical and management drivers

At the plot-scale, NO emissions were sensitive, by increasing order, to: soil type, crop type (including fertilizer N rates), climate and soil microbiological parameters. The marginal distributions of NO emissions with fixed climate or crop type were relatively homogeneous, and resembled the overall distribution of this variable (see boxplots of Fig. 2a–c). Conversely, the marginal distributions related to soil types were more dissimilar and differed from the overall distribution, evidencing a strong influence of this factor on NO emissions (Fig. 2b). In particular, emission rates were markedly higher with the Luvisols, which tended to have higher water contents than sandy Podzosols. The analysis of variance allowed us to quantify the weights of the main factors and their interactions (Monod et al., 2006), and its results are presented in Table 3. The sensitivity indices of the main factors explained 82.5% of the total variance of NO emissions, while first-order interactions between factors accounted for 17.4% of it (the residual variance was thus negligible). Soils were by far the most influential factors, and its interactions with crops was the most significant term. Crop type explained 4% of total variance, and the other factors appeared negligible since they only explained 1% of the variance (Table 3).

At the regional scale, spring crops released more NO than winter crops due to higher soil temperatures after fertilizer applications and slower uptake of fertilizer N after sowing. The mean topsoil temperatures in March, April and May 2001 were 8.5, 10.3 and 16.2 °C, respectively. Since NO emissions respond to temperature with a Q_{10} function of 2.1 in the model, this means a potential factor of 2.1 for NO fluxes between the fertilization period of wheat (March, see Table 1) and maize (late April). The response of NO emissions to fertilizer rates was remarkably linear (with R^2 values above 0.99), with higher slopes (corresponding to emission factors) for the maize (2.6%) than for the wheat (1.9%). For both crops, background NO emissions totaled 2.6 kg N ha^{-1} over simulation period.

3.2. Time course of NO emissions

Fig. 4a–b compares the dynamics of NO emissions under winter and spring crops, and for 5 soil types with contrasted

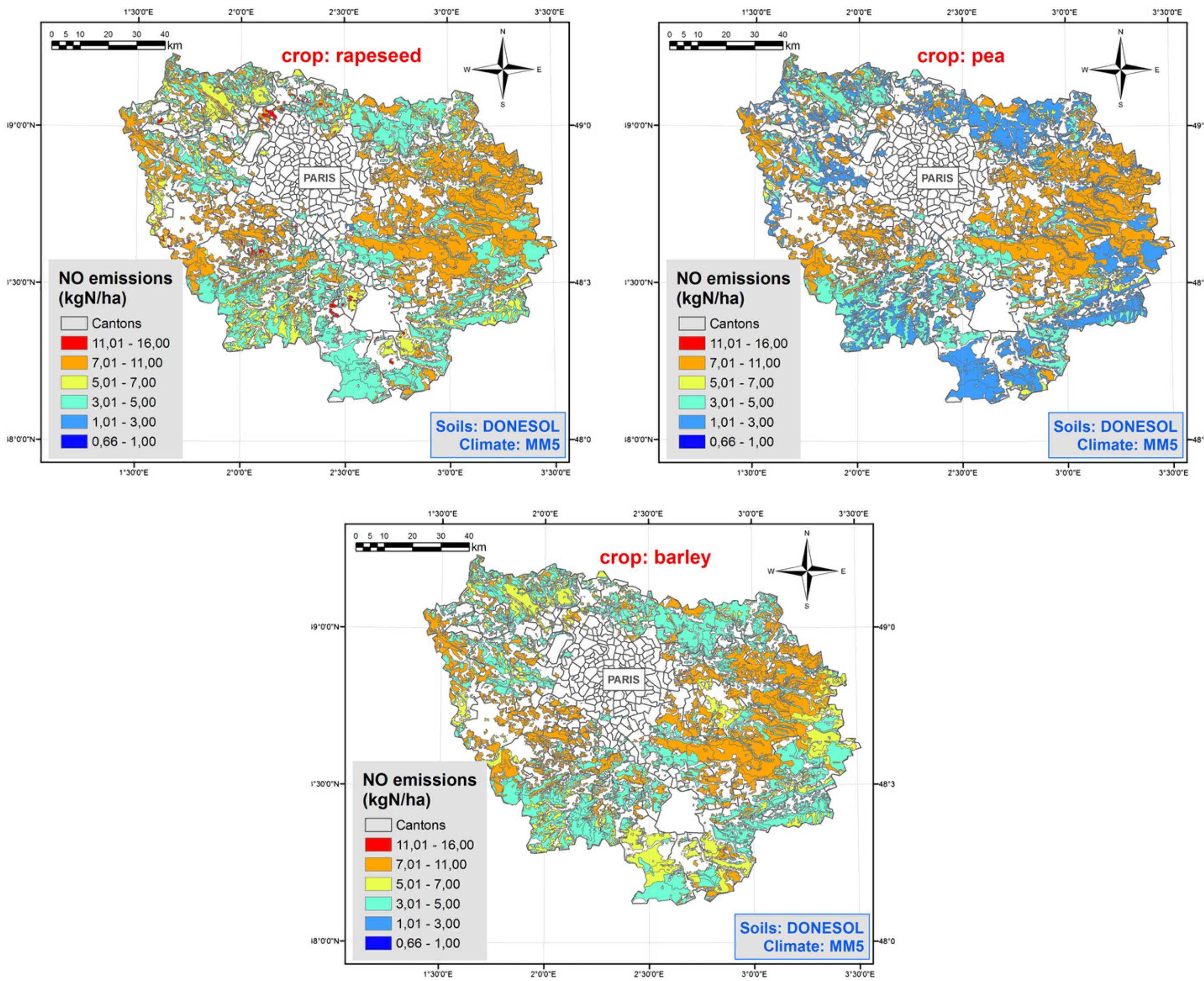

Fig. 6. Maps of cumulated NO emissions from November 2000 through December 2001, for 3 crop types.

hydrodynamic regimes. Soil and crop types had a clear impact on the emission patterns, as a result of strong differences in some of their environmental drivers (Fig. 4c–h). In spring, the magnitude of NO emissions under the maize crop was higher than the wheat crop after fertilization due to higher N application rates, soil temperature and optimal soil moisture content (corresponding to 60% water-filled pore space - WFPS; Linn and Doran, 1984). Conversely, WFPS ranged from 60 to 90% around fertilizer applications for the wheat, resulting in reduced nitrification activity. Also, fertilizer N was input as a single application upon sowing for the maize, at a time when there was no demand from the plants. Most of the NO emissions happened in the month following sowing, before the plants started growing and taking up fertilizer N. Towards the end of the summer, both wheat and maize had similar NO emissions, due to the mineralization of soil organic matter and similar soil environmental conditions (see Fig. 4). Throughout autumn and winter, mineralization slowly decreased due to decreasing soil temperature, and NO emissions reached a stable background level of few g N–NO ha^{-1} d^{-1}. There were further reduced by sub-optimal soil moisture content, the latter being either too low in autumn or too high in winter.

The sensitivity to soil types is mostly related to differences in their soil water-filled pore space (WFPS) dynamics (Fig. 4). Typical Luvisols produced higher NO peaks than the hydromorphic soils (hydromorphic Luvisols and Planosols), or than the cherty Calcosols, because they were well-drained and their water balance led to optimal soil moisture content for nitrification upon fertilizer applications in spring. The WFPS of hydromorphic soils tended to remain above the optimum for nitrification, which hampered this process at that time. However, during the rest of the simulation period, the hydromorphic Luvisols emitted more NO than the other Luvisols whatever the crop, due to higher WFPS, and their efflux totaled 8.6 g N–NO ha^{-1} d^{-1} compared to 6.2 g N–NO ha^{-1} d^{-1} for the latter.

3.3. Spatial distribution of NO emissions over Ile de France

Figs. 5 and 6 map NO emissions over the various crops simulated, as cumulated over the 14-month simulation timeframe. Emissions were larger over spring crops (maize and surgarbeet) than winter crops (wheat, barley and rapeseed), pea-cropped and fallow soils being the weakest emitters due to the absence of mineral fertilizer application. A large heterogeneity in NO

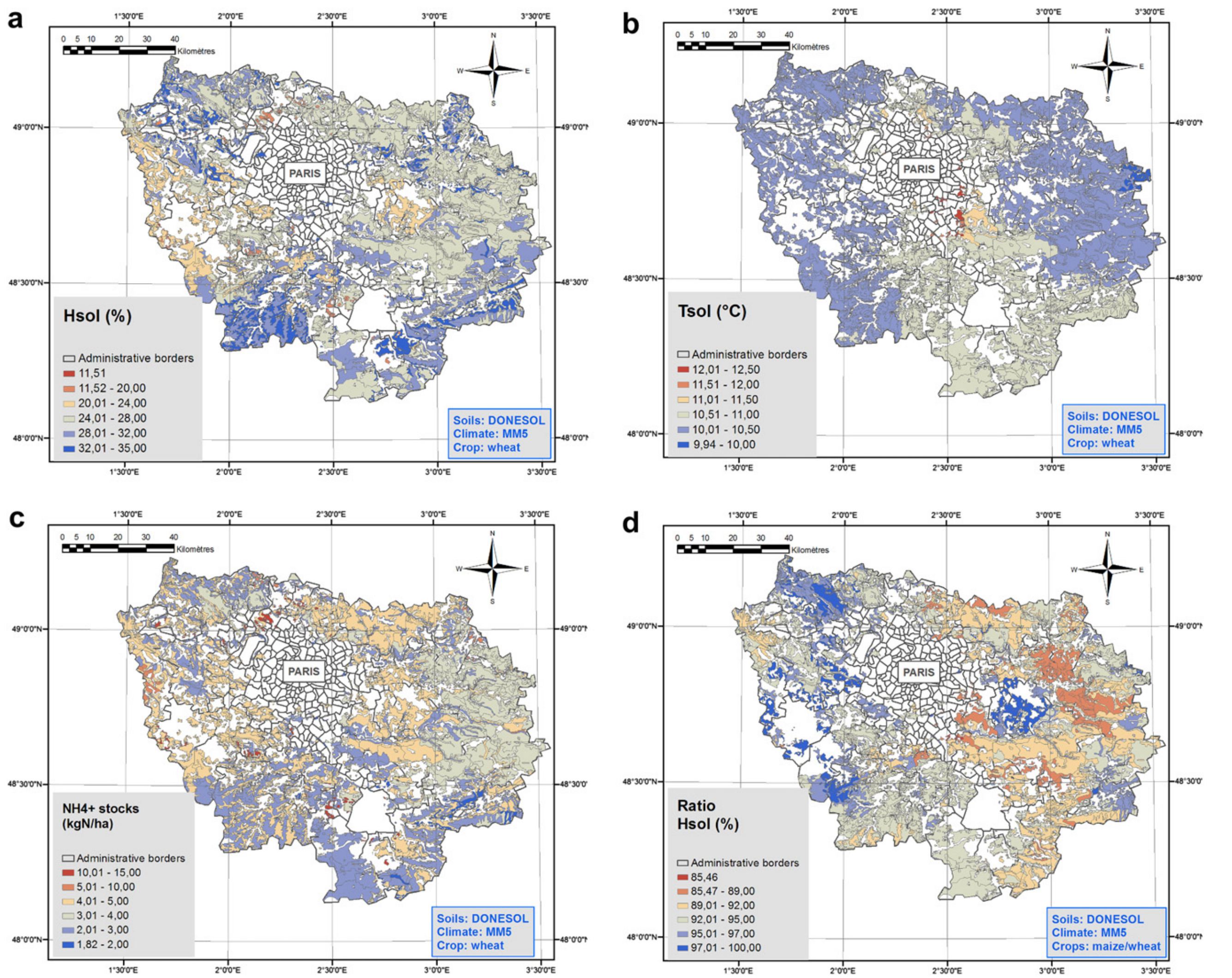

Fig. 7. Emission drivers simulated by CERES-EGC: time-averaged soil moisture, in volumetric percents (a), soil temperature (b), and soil ammonium content (c) under a winter wheat crop. Map (d) displays the ratio of soil moisture contents under spring maize and winter wheat.

emissions may be noted on all maps: the fluxes ranged between 2.8 and 16.5 kg N–NO ha^{-1} for the spring crops, with a median value of 4.9 kg N–NO ha^{-1}, whereas the range was 2.3–10.1 kg N–NO ha^{-1} for winter crops, with a median of 3.8 kg N–NO ha^{-1}. Lastly, for the crops without fertilizer application values are comprised between 0.66 and 9.3 kg N–NO ha^{-1}, with a median value of 2.8 kg N–NO ha^{-1}. There were consistent emission pattern across the maps, with largest emissions occurring to the East of the domain, and to a lesser proportion in its Southern and South-Western parts. This pattern was strongly linked with the regional distribution of soils (Fig. 1), inasmuch as they influenced the physical drivers of nitrification. The latter include soil temperature, soil moisture and ammonium contents (Laville et al., 2005), whose regional distributions are depicted on Fig. 7.

Soil moisture content was highly variable across the region, as a result of the heterogeneity in soil types and rainfall. The Podzosols, with sandy texture, presented the lowest levels of soil moisture, appearing as red and orange spots to the South-East of Paris (Fig. 7a). Intermediate levels of soil moisture were simulated for the various types of Luvisols around Paris, with a drier fringe along the southwestern limit corresponding to well-drained soils. Hydromorphic Luvisols, located mostly in the eastern part of the domain had a moisture content ranging from 50 to 70% of water-filled pore space (WFPS) in the spring months, which was close to the optimum for nitrification (60% WFPS), resulting in high NO emissions. Neoluvisols had the highest moisture contents, ranging from 55 to 70% WFPS, and had slightly lower NO fluxes than the hydromorphic Luvisols. Spring crops resulted in drier soil conditions than winter crops, with a relative difference reaching up to 15% over the simulation timeframe (Fig. 7d).

Soil temperature was much more homogeneous than soil moisture over the region, mostly varying within a 1 °C band. This would result in a less than 5% relative difference in the NO fluxes, given the temperature response function assumed in the model, and had little impacts on regional variability. Time-averaged soil ammonium stocks (the subtrate of nitrification) varied within a wider range, from 2 to more than 10 kg N ha^{-1}, but were not directly related to NO emission patterns. This may result from the strong seasonal dynamics of soil ammonium (Fig. 5), which implies that the yearly average ammonium content of soils hardly reflects the peak NO emissions in spring.

Other more constant soil properties may control nitrification activity and NO emissions, such as soil pH and texture (Yan et al., 2005). They are not taken into account in the CERES-EGC model, as discussed in its field-scale tests (Rolland et al., 2008), but this

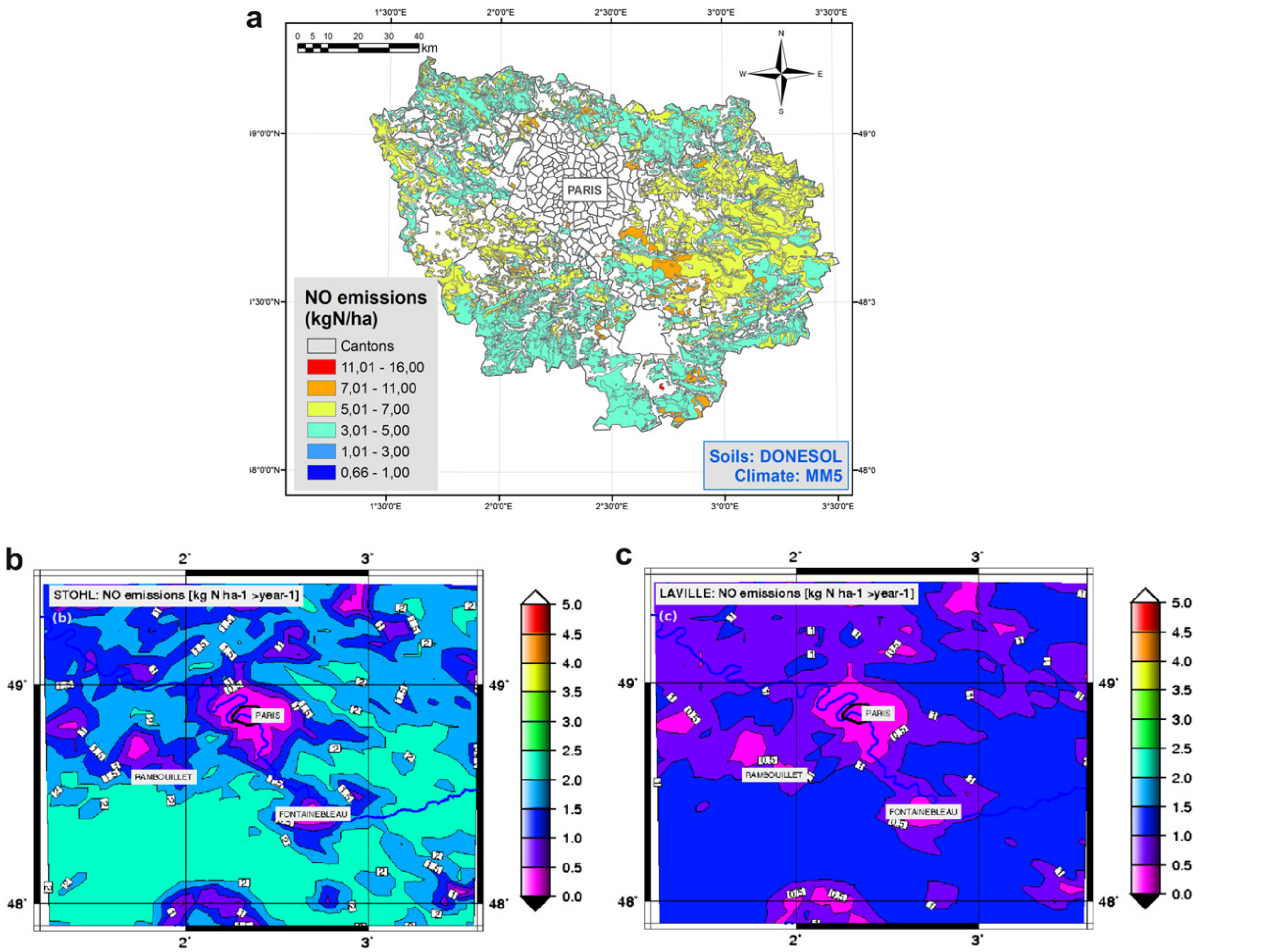

Fig. 8. Maps of cumulative NO emissions from arable soils (kg N-NO ha^{1} yr^{-1}), as estimated by our spatial inventory (a), by the Stohl et al. (1996) model (b) and by the Laville et al. (2005) model (c), from November 2000 to December, 31st 2001.

probably resulted in a partial rendering of soil variability effects on NO emissions.

Regarding the resolution of soil or climate maps, the regional distribution of soils appeared as a major driver in the spatial patterns of NO fluxes (Fig. 3a–c). In the simulation with uniform soil type (Neoluvisol) across the region, the spatial distribution of NO emissions was nearly homogeneous and close to the flux corresponding to the Neoluvisol and Grignon meterologica data combination (in the 250–300 g N–NO ha^{-1} range). In the climate forcing output by MM5, annual rainfall ranged from 400 to 1200 mm and daily air temperatures varying within a 25% band across the region, the Grignon station being in the upper range for these variables. However, these stark heterogeneities only exerted a marginal effect on NO emissions compared to soil variability.

3.4. Comparison with other estimates

According to our simulations, NO emissions from agricultural soils averaged 5.1 kg N–NO ha^{-1} between November 2000 and December 2001, and ranged from 1.47 to 11.1 kg N–NO ha^{-1}. Since the mean fertilizer application rate was 150 kg N–NO ha^{-1}, we could estimate an aggregated emission factor of 1.7% for Ile de France, after subtracting the background flux of 2.6 kg N–NO ha^{-1}. Fig. 8 compares our NO emission maps with those currently implemented in the chemistry-transport model CHIMERE, based on either the Stohl et al. (1996) NO algorithm or the Laville et al. (2005) model. For the same time period, these models yielded emissions ranging from 0.5 to 2.5 kg N–NO ha^{-1}, and from 0.5 to 1.5 kg N–NO ha^{-1}, respectively. An explanation for these rates being lower than ours may be that background NO emissions (*i.e.* emissions in the absence of fertilization) are smaller in magnitude with these algorithms. The spatial distribution of cropland sources was more homogeneous with the CHIMERE algorithms than with ours, because the latter are only based on a single land-cover class (arable land) which does not take soil type into account (Fig. 8). In our approach, as showed in the previous section, the variability of soil types had a strong effect on NO emissions.

We compared the regional total of 2761.0 t N–NO simulated by CERES-EGC over the 14-month timeframe with other inventories. Since the contribution of the 2 last months of 2000 was approximately 5%, this translates as an annual total of 2623 t N–NO. The national inventory of atmospheric pollutants in France (CITEPA, 2008) estimates the contribution of agricultural soils based on emission factors specific to N fertilizer forms FAO/IFA (2001), and on fertilizer delivery data. The resulting estimate for Ile de France is 404.3 t N–NO yr^{-1}, which may be compared to our estimate by adding the background emissions (1328.4 t NO_2 yr^{-1}), yielding a total of 1838.2 t N–NO yr^{-1}, 30% lower than our estimate. Using an approach similar to ours, Butterbach-Bahl et al. (2004) predicted average NO emission rates of 8.6 kg N–NO ha^{-1} yr^{-1} for arable crops in the Saxony region of Germany, which is of similar magnitude as our regional mean. A more recent EU-wide simulation with the same methodology resulted in a much lower range for the Ile de France area, with soil emission rates varying from 1 to 1.5 kg N–NO ha^{-1} yr^{-1} (Butterbach-Bahl et al., 2009), ie 4 times less than our average. This may have been an effect of inter-annual climate variability, since the simulations were run for the year 2000, compared to 2001 in our case, but both years had similar annual rainfall (869 and 765 mm, resp.) and mean air temperature (11.4 and 11.1 °C). Fertilizer N rates were also very similar between their study and ours. This gap is more probably due to the DNDC model under-estimating the mean observed NO fluxes by a factor of 4 in the Grignon experimental test site, located in western Ile de France, whereas CERES-EGC achieved a relative mean deviation of 20% on the same data set (Rolland et al., 2008).

Lastly, we checked our bottom-up estimate of N fertilizer inputs to arable crops against the total input that may be approximated from the fertilizer delivery data in Ile de France. In 2001, the latter amounted to 70 229 t of fertilizer N. In our approach, based on agricultural statistics and field surveys of management practices, the average fertilization rate was about 150 kg N ha^{-1} (see Table 1), and arable crops covered 573590 ha. Thus, the total fertilizer input was estimated at 86 038 t N, which is within 18% of the UNIFA estimate. Thus, simulating the dominant crops in the region enabled us to account for the overall use of fertilizer N in agriculture.

4. Conclusion

Although biogenic NO emissions may significantly contribute to photochemical processes in rural and urban areas (Stohl et al., 1996), little work has tested or discussed the possible influence of a finer-scale description for them in the context of atmospheric chemistry modeling (Cortinovis, 2004; Rolland, 2008). Here, we produced a high-resolution (kilometric level) emission map of NO emissions from cropland over the Ile de France region using an agro-ecosystem model and GIS databases of environmental and management drivers.

Regional year-round NO emissions totaled 2623 t N–NO yr^{-1} over the whole region, and ranged from 1.4 to 10.5 kg N–NO ha^{-1} across the various spatial simulation units. The overall emission factor for fertilizer-derived NO emissions was 1.7%, while background emissions contributed half of the total NO efflux. Our results underlined the importance of taking the spatial distribution of soils into account, since they were the major drivers behind the spatial patterns of arable sources. Regarding management effects, spring crops had 35% higher emissions than winter crops, due to more conducive temperature conditions upon fertilizer application. Compared to simpler approaches based on fixed emission factors (as currently used in chemistry-transport models), ecosystem models have the advantages of eliciting the effect of soil type, land-use, crop management and their interactions with climate. They thus have the potential to improve emission maps at regional and national level, and air quality prediction by chemistry-transport models. In the future, important controls such as soil pH and canopy effects should be taken into account, along with the contribution of denitrification to NO emissions, to produce more accurate simulations of agricultural sources.

Acknowledgments

M.-N. Rolland was supported by the French Environmental Agency (ADEME) and the French National Institute for Agricultural Research (INRA). We would like to thank an anonymous referee for her/his help in improving the manuscript.

References

Agreste – Service Central d'Enquêtes et d'Etudes Statistiques, 2001. Enquête sur les Pratiques Culturales en 2001. Chiffres et données. Série Agriculture 159, French Ministry of Agriculture. Forestry and Fisheries, Paris.

Baize, D., Girard, M.-C., 1998. A Sound Reference Base for Soils: the Référentiel Pédologique (Text in English. Translation by J.M. Hodgson, N.R.Eskenazi, D. Baize, Trans.). INRA Éditions, Paris.

Bardossy, A., Plate, E.J., 1992. Space time model for daily rainfall using atmospheric circulation patterns. Water Resources Research 28, 1247–1259.

Butterbach-Bahl, K., Strange, F., Papen, H., Li, C., 2001. Regional inventory of nitric oxide and nitrous oxide emissions for forest soils of southeast germany using the biogeochemical model PnET-N-DNDC. Journal of Geophysical Research 106, 155–166.

Butterbach-Bahl, K., Kesik, M., Mielhe, P., Papen, H., Li, C., 2004. Quantifying the regional source strength of N-trace gases across agricultural and forest ecosystems with process-based models. Plant and Soil 260, 225–243.

Butterbach-Bahl, K., Kahl, M., Mykhayliv, L., Werner, C., Kiese, R., Li, C., 2009. A European-wide inventory of soil NO emissions using the biogeochemical models DNDC/Forest-DNDC. Atmospheric Environment 43, 1392–1402.

Chapman, L., Thornes, J.E., 2003. The use of geographical information systems in climatology and meteorology. Progress in Physical Geography 27, 313–330.

Centre Interprofessionnel Technique d'Etudes de la Pollution Atmospherique (CITEPA), 2008. Inventaire des Emissions de Polluants Atmosphériques en France – Séries Sectorielles et Analyses Etendues. CITEPA, Paris.

Cortinovis, J., 2004. Field-monitoring and modeling of biogenic emissions of nitrogen oxides and isoprene from natural and managed ecosystems: impact on tropospheric ozone. Ph.D. Dissertation, Paul Sabatier University, Toulouse, France (in French).

Davidson, E.A., Kingerlee, W., 1997. A global inventory of nitric oxide emissions from soils. Nutrient Cycling in Agroecosystems 48, 37–50.

Deguillaume, L., Beekmann, M., Derognat, C., 2008. Uncertainty evaluation of ozone production and its sensitivity to emission changes over the Ile-de-France region during summer periods. Journal of Geophysical Research 113, D02304. doi:10.1029/2007JD009081.

Delmas, R., Serça, D., Jambert, C., 1997. Global inventory of NO_x sources. Nutrient Cycling in Agroecosystems 48, 51–60.

Dudhia, J., 1993. A nonhydrostatic version of the Penn State/NCAR mesoscale model: validation tests and simulation of an Atlantic cyclone and cold front. Monthly Weather Review 121, 1493–1513.

Faivre, R., Leenhardt, D., Voltz, M., Benoît, M., Papy, F., Dedieu, G., Wallach, D., 2004. Spatialising crop models. Agronomie 24, 205–217.

Food and Agriculture Organization (FAO)/International Fertilizer Industry Association (IFIA), 2001. Global Estimates of Gaseous Emissions of NH3, NO and N2O from Agricultural Land. Rome, Italy.

Gabrielle, B., Denoroy, P., Gosse, G., Justes, E., Andersen, M.N., 1998. A model of leaf area development and senescence for winter oilseed rape. Field Crops Research 57, 209–222.

Gabrielle, B., Roche, R., Angas, P., Cantero-Martinez, C., Cosentino, L., Mantineo, M., Langensiepen, M., Hénault, C., Laville, P., Nicoullaud, B., Gosse, G., 2002. A priori parametrisation of the CERES soil-crop models and tests against several European data sets. Agronomie 22, 25–38.

Gabrielle, B., Laville, P., Hénault, C., Nicoullaud, B., Germon, J.C., 2006a. Simulation of nitrous oxide emissions from wheat-cropped soils using CERES. Nutrient Cycling in Agroecosystems 74, 133–146.

Gabrielle, B., Laville, P., Duval, O., Nicoullaud, B., Germon, J.-C., Hénault, C., 2006b. Process-based modelling of nitrous oxide emissions from wheat-cropped soils at the sub-regional scale. Global Biogeochemical Cycles 20, GB4018.

Godde, M., Conrad, R., 2000. Influence of soil properties on the turnover of nitric oxide and nitrous oxide by nitrification and denitrification at constant temperature and moisture. Biology and Fertility of Soils 32, 120–128.

Hermel, K., 2001. Comparaison des bilans environnementaux entre différents systèmes d'agriculture. M.Sc. dissertation, Ecole Nationale Supérieure des Mines de Paris, Paris.

Institut Français de l'Environnement (IFEN), 2005. CORINE land cover 2000 for France. Technical report, Orléans, France.

Kiese, R., Li, C., Hilbert, D.W., Papen, H., Butterbach-Bahl, K., 2004. Regional application of Pnet-n-DNDC for estimating the N_2O source strength of tropical rainforests in the wet tropics of Australia. Global Change Biology 11, 128–144.

King, D., Daroussin, J., Jamagne, M., 1994. Proposal for a spatial organization model in soil science (the example of the European Communities soil map). Journal of American Society for Information Science 45, 705–717.

Laville, P., Hénault, C., Gabrielle, B., Serça, D., 2005. Measurement and modelling of NO fluxes on maize and wheat crops during their growing seasons: effect of crop management. Nutrient Cycling in Agroecosystems 72, 159–171.

Li, C., Mosier, A., Wassmann, R., Cai, Z., Zheng, X., Huang, Y., Tsuruta, H., Boonjawat, J., Lantin, R., 2004. Modeling greenhouse gas emissions from rice-based production systems: sensitivity and upscaling. Global Biogeochemical Cycles 18, GB1043.

Linn, D.M., Doran, J.W., 1984. Effect of water-filled pore space on carbon dioxide and nitrous oxide production in tilled and nontilled soils. Soil Science Society of America Journal 48, 1667–1672.

Monestiez, P., Courault, D., Allard, D., Ruget, F., 2001. Spatial interpolation of air temperature using environmental context: application to a crop model. Environmental and Ecological Statistics 8, 297–309.

Monod, H., Naud, C., Makowski, D., 2006. Uncertainty and sensitivity analysis for crop models. In: Wallach, D., Makowski, D., Jones, J.W. (Eds.), Working with Dynamic Crop Models. Elsevier, Amsterdam, pp. 55–99.

Penman, H.L., 1948. Natural evaporation from open water, bare soil and grass. Proceedings of the Royal Society of London, Series A, Mathematical and Physical Sciences 193, 120–145.

Roche, R., Gabrielle, B., Bouthier, A., Gosse, G., 2001. Modelling of nitrate leaching in rapeseed-wheat rotations. In: Donatelli, M. (Ed.), Modelling Cropping Systems. Proc. ESA Congress, July 2001, Florence, Italy, pp. 175–176.

Rolland, M.-N., 2008. Biophysical modelling of NO emissions by crops, spatialization and impact on photochemical ozone formation at regional scale. Ph.D. Dissertation, Paris 6 University, Paris (in French). *URL:* http://tel.archives-ouvertes.fr/tel-00325316/en/

Rolland, M.-N., Gabrielle, B., Laville, P., Serça, D., Cortinovis, J., Larmanou, E., Lehuger, S., Cellier, P., 2008. Modeling of nitric oxide emissions from temperate agricultural soils. Nutrient Cycling in Agroecosystems 80, 75–93.

Simpson, D., Winiwarter, W., Borjesson, G., Cinderby, S., Ferreiro, A., Guenther, A., Hewitt, C.N., Janson, R., Khalil, M.A.K., Owen, S., Pierce, T.E., Puxbaum, H., Shearer, M., Steinbrecher, S., Svennson, B.H., Tarrason, L., Oquist, M.G., 1999. Inventorying emissions from nature in Europe. Journal of Geophysical Research 104, 8113–8152.

Skiba, U., Sozanska, M., Metcalfe, S., Fowler, D., 2001. Spatially disaggregated inventories of soil NO and N_2O emissions for Great Britain. Water, Air, and Soil Pollution: Focus 1, 109–118.

Stohl, A., Williams, E., Kromp-Kolb, G.W.H., 1996. An European inventory of soil nitric oxide emissions and the effect of these emissions on the photochemical formation of ozone. Atmospheric Environment 30, 3741–3755.

Yan, X., Ohara, T., Akimoto, H., 2005. Statistical modelling of global soil NO_x emissions. Global Biogeochemical Cycles 19, GB3019. doi:10.1029/2004GB002276.

Yienger, J.J., Levy, H., 1995. Empirical model of global soil-biogenic NOx emissions. Journal of Geophysical Research 100, 11447–11464.